Heliyon 10 (2024) e36241

Contents lists available at ScienceDirect

Heliyon

journal homepage: www.cell.com/heliyon

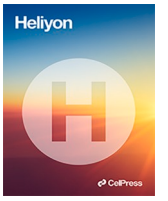

Research article

Network pharmacology and *in vivo* experimental studies reveal the protective effects of 6-hydroxygenistein against hypobaric hypoxia-induced brain injury

Zhiqun Shi [a,b], Jie Zhang [a], Huiping Ma [b], Linlin Jing [a,b,*]

[a] Department of Pharmacy, the First Affiliated Hospital of Xi'an Jiaotong University, Xi'an, Shaanxi, 710061, China
[b] Department of Pharmacy, the 940th Hospital of Joint Logistics Support Force of PLA, Lanzhou, Gansu, 730050, China

ARTICLE INFO

Keywords:
6-Hydroxygenistein
Hypobaric hypoxia
Brain injury
Network pharmacology
Molecular mechanism
Oxidative stress
Inflammatory response

ABSTRACT

Hypobaric hypoxia-induced brain injury (HHBI) is a progressive neurodegenerative disease that has still not been effectively treated. There are several different mechanisms involved in HHBI. Among them, oxidative stress and inflammation response predominate. 6-hydroxygenistein (4′,5,6,7-tetrahydroxyisoflavone, 6-OHG) is a hydroxylated derivative of genistein with excellent antioxidant activity, however, the protective effects and underlying mechanisms against HHBI have not been clarified. In the present study, we aimed to explore the mechanisms of action of 6-OHG on HHBI using network pharmacology and experimental validation. Network pharmacology analysis revealed 186 candidate targets through the intersection of the targets of 6-OHG and related genes in HHBI, which were mainly enriched in oxidative stress and inflammation response. Moreover, key targets of 6-OHG against HHBI, namely Nrf2 and NF-κB, were screened and found to be closely related to oxidative stress and inflammation response. Subsequent *in vivo* experiments revealed that 6-OHG treatment attenuated oxidative stress and inflammation response, prevented energy disorder and apoptosis as well as maintained the BBB integrity in HHBI mice. In addition, 6-OHG administration up-regulated the expressions of Nrf2 and HO-1 and down-regulated the expressions of NF-κB and NLRP3, thereby inhibiting oxidative stress and inflammation response. Hence, the present study demonstrates that 6-OHG protects against HHBI by stimulating the Nrf2/HO-1 signaling pathway and suppressing the NF-κB/NLRP3 signaling pathway.

1. Introduction

Plateaus are widely distributed in the world, accounting for about 45 %. At high altitudes, a decrease in oxygen (O_2) partial pressure creates a unique environmental condition known as hypobaric hypoxia (HH) [1], which results in a series of physiological and pathological changes in humans and animals [2,3]. Brain is especially vulnerable to HH due to its high basal metabolic rate and oxygen consumption [4]. HH is capable of inducing brain damage, primarily characterized by headaches, cognitive impairment, and even high altitude cerebral edema (HACE), which can be life-threatening [5,6]. However, effective interventions are still limited. In recent year, there has been a significant increase in the number of people going to high altitude, which makes hypobaric hypoxia-induced brain

* Corresponding author. Department of Pharmacy, the First Affiliated Hospital of Xi'an Jiaotong University, NO.277 Yanta West Road, Yanta District, Xi'an, Shanxi, 710061, China.
E-mail address: jinglinlin@xjtufh.edu.cn (L. Jing).

https://doi.org/10.1016/j.heliyon.2024.e36241
Received 4 May 2024; Received in revised form 12 August 2024; Accepted 13 August 2024
Available online 14 August 2024

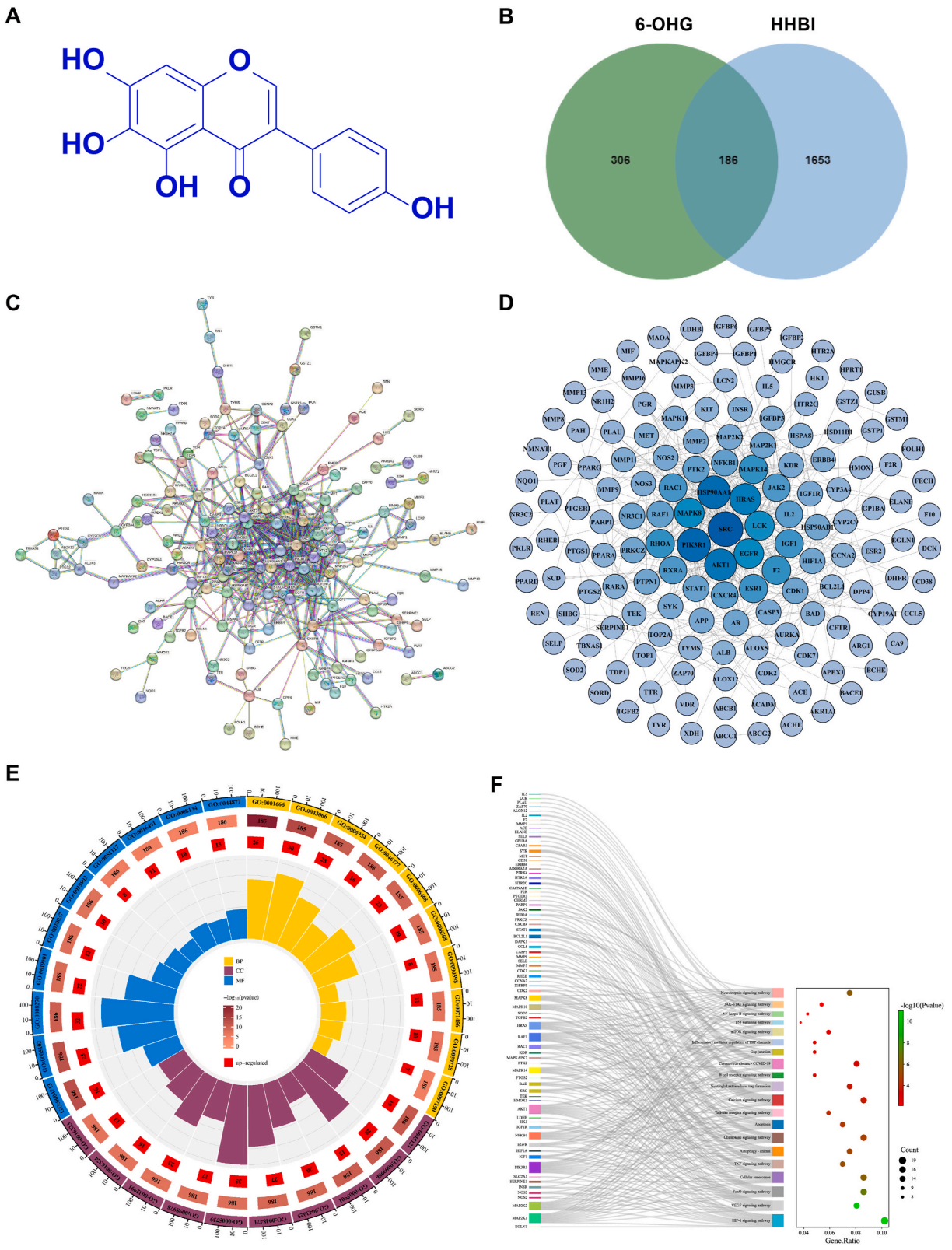

Fig. 1. Network pharmacology analysis of 6-OHG against HHBI. (A) Chemical structure of 6-OHG. (B) Venn diagram of potential targets. (C, D) The protein-protein interaction network map of 183 target genes. (E) Analysis of GO biological function enrichment for 6-OHG-treated HHBI. (F) Analysis of KEGG pathway enrichment for 6-OHG-treated HHBI.

injury (HHBI) received growing attention.

HH can lead to a rise in reactive oxygen species (ROS) primarily originating from impaired mitochondrial respiration and reactive nitrogen species (RNS) mainly produced via excess nitric oxide (NO), and inhibition of antioxidant enzymes activities, which perturb redox homeostasis, ultimately leading to oxidative stress [7]. Numerous studies have shown that oxidative stress contributes to neuronal damage induced by HH [8–10]. In addition, HH exposure may be related to inflammatory response, which further exacerbates neuronal impairment [11]. Accordingly, treatment with agents with antioxidant and/or anti-inflammatory activities can prevent HHBI.

6-hydroxygenistein (4′,5,6,7-tetrahydroxyisoflavone, 6-OHG, Fig. 1A) is a hydroxylated derivative of genistein with ortho-dihydroxyl groups in its structure and exhibits anticancer [12], antimelanogenesis [13], and hepatoprotective [14] activities. However, these results are achieved via *in vitro* studies. A major reason may be the difficulty in obtaining adequate amounts of 6-OHG, because it is only found in fermented soybean foods or microbial fermentation broth and the content is extremely rare [15]. To address this issue, we established a simple synthesis method using genistein as starting material [16], which could supply enough quantity for animal experiments *in vivo*. In addition, we also proved that 6-OHG exhibited remarkable antioxidant and free radical scavenging activity [16]. However, whether 6-OHG may inhibit HHBI and its underling mechanism is not yet known.

Network pharmacology proposed by Hopkins in 2008 is a scientific method to predict molecular targets through systems biology and network analysis [17]. There is growing evidence that network pharmacology has been widely applied to explore the mechanism of drugs against disease [18].

In the current study, we first confirmed the protective effect of 6-OHG against HHBI using a HH mice model and then elucidated the underling mechanism via integrated network pharmacology and experimental validation. The results will pave the way for developing 6-OHG as a drug for prevention and therapy of HHBI.

2. Materials and methods

2.1. Network pharmacology research

2.1.1. Prediction of potential targets of 6-OHG on HHBI

We searched for the targets of 6-OHG by the Swiss Target Prediction (SWP, https://www.SwissTargetPrediction.ch) platform, Traditional Chinese Medicine Systems Pharmacology Database and Analysis Platform (TCMSP, https://old.tcmsp-e.com/tcmsp.php), PharmMapper (http://www.lilab-ecust.cn/pharmmapper/), superPred (https://prediction.charite.de/) databases and Similarity ensemble approach (SEA, https://sea.bkslab.org/). HHBI-related targets were collected from databases including the GeneCards database (https://www.genecards.org/) and the Online Mendelian Inheritance in Man (OMIM) database (https://www.omim.org/) using "high altitude brain injury" and "hypobaric hypoxia brain injury" as the keywords. The intersection targets of 6-OHG and HHBI were obtained via VENNY2.1 (https://bioinfogp.cnb.csic.es/tools/venny/).

2.1.2. Protein interaction network construction and analysis

The protein-protein interaction (PPI) network diagram was acquired via importing the potential targets into the Retrieval of Interacting Genes/Proteins (STRING) database (https://www.string-db.org/). The organism was chosen as *Homo sapiens*, and targets with interaction scores $\geq$0.900, hiding the free nodes and download the protein correlation information were selected as the final targets. The TSV-format file was obtained from the STRING database and imported into Cytoscape 3.7.2 for core target screening.

2.1.3. Enrichment analysis of gene ontology (GO) and the kyoto encyclopedia of genes and genomes (KEGG)

The pathways of 6-OHG for the treatment of HHBI were identified utilizing the Database for Annotation, Visualization, and Integrated Discovery (DAVID) v6.8 (https://david.ncifcrf.gov/). The cut-off criterion of the DAVID analysis was p value less than 0.05, which was regarded as statistical significance. Simultaneously, the intersecting targets underwent GO and KEGG pathway enrichment analysis. Three aspects, including biological process (BP), molecular function (MF), and cellular components (CC) were involved in GO analysis.

2.1.4. Molecular docking analysis

The structure of 6-OHG was retrieved from PubChem (https://pubchem.ncbi.nlm.nih.gov/). The crystal structures of NF-κB (PDB ID:3GUT), NLRP3 (PDB ID:7ALV), Nrf2 (PDB ID: 5WHO) and HO-1(PDB ID: 3TGM) were retrieve from the Protein Data Bank database (https://www.rcsb.org/) and exported in PDB format. The receptor proteins were dehydrated and ligands were eliminated using PyMOL2.0. Then the receptor protein was docked with the 6-OHG using AutoDock Vina 1.1.2. The affinity scores were employed to assess the binding potential between 6-OHG and the target protein.

2.2. In vivo experimental study

2.2.1. Chemicals and reagents

6-OHG was synthesized according to our previously reported method [16]. Primary antibodies against NF-κB p65, p-NF-κB p65, Myd88, IκB-α, and p-IκB-α were supplied by Cell Signaling Technology, Inc. (Danvers, MA, United States). Primary antibodies against IL-6, TNF-α, NLRP3, Nrf2, HO-1, Bax, Bcl-2, Cleaved Caspase-3 and β-actin were provided by Abcam (Cambridge, UK). Secondary antibodies were obtained from ZSGB-BIO (Beijing, China).

2.2.2. Experimental animals

Male Balb/c mice (6–8 weeks old, weight 18–22 g, SPF rank) were provided by the Beijing SBF Biotechnology Co., Ltd (Beijing, China). The experimental animal production number and the experimental animal use number were SCXK (Jing) 2019-0010 and SYXK (Jun) 2014-0029, respectively. The mice were housed at 23 ± 2 °C with a 12 h light-dark cycle and *ad libitum* accessed to a standard diet and water, and acclimatized to the facilities for one week before experiments. All animal study was performed according to the Guide for the Care and Use of Laboratory Animals (NIH Publications No. 8023, revised 2011). The animal protocol was reviewed and approved by the Animal Care and Use Committee of 940th Hospital (No: 2021KYLL241).

2.2.3. Normobaric hypoxia test

The normobaric hypoxia test was conducted based on our earlier published method [19]. Fifty male Balb/c mice were randomly allocated into five groups (n = 10 per group): hypoxia group, acetazolamide group (200 mg/kg, positive control), and three 6-OHG groups (25, 50 or 100 mg/kg). The acetazolamide and 6-OHG were injected intraperitoneally to mice as a suspension. The mice in the hypoxia group were injected intraperitoneally with normal saline (0.2 mL/20 g). Thirty minutes after administration, mice were subjected to the normobaric hypoxia test. The survival time of mice was documented and the prolongation rate was calculated according to the following formula: Prolongation rate (%) = (survival time of treatment group/survival time of hypoxia group - 1) × 100.

2.2.4. Acute decompression hypoxia tolerance test

The acute decompression hypoxia tolerance test was conducted based on our earlier published method [19]. Fifty male Balb/c mice were randomly allocated into five groups (n = 10 per group), namely the acute decompression group (normal saline, 0.2 mL/20 g), acetazolamide group (200 mg/kg), and three 6-OHG groups (25, 50 or 100 mg/kg). Thirty minutes after intraperitoneal injection, the mice were placed in a low-pressure oxygen cabin (FLYDMC50-IIC, Guizhou FengLei, China). The altitude was increased to 5000 m and 8000 m at a decompression rate of 20 m/s and held for 5 min each, then the altitude was finally increased to 10 000 m. The mortality rate of mice within 1 h was observed and counted.

2.2.5. Acute hypobaric hypoxia test

The acute hypobaric hypoxia experiment was conducted based on our earlier published method [19]. Thirty nine male Balb/c mice were randomly allocated into three groups (n = 13 per group): the normoxia group, hypobaric hypoxia (HH) group, and HH + 6-OHG (100 mg/kg) group. The 6-OHG was administered by intraperitoneal injection. The mice in the normoxic group and HH group were injected intraperitoneally with normal saline (0.2 mL/20 g). Thirty minutes after administration, mice in HH and HH + 6-OHG groups were exposed to an altitude of 8000 m (8 % O_2, 0.035 MPa) by placing them in an experimental animal cabin of simulated high-altitude environment (DYC-3070, Guizhou FengLei, China). Temperature and humidity in the cabin were controlled at 25 ± 2 °C and 45 ± 5 %, respectively. The mice were sacrificed by cervical dislocation after 24 h of exposure. To avoid hypoxia and reoxygenation injury at low altitude, they were euthanized at an altitude of 4000 m. Serum and brain samples was collected and stored at −80 °C for further analysis.

2.2.6. Haematoxylin and eosin (HE) staining

Brain tissues of three mice in each group were fixed in 4 % paraformaldehyde for 24 h and used for histological analysis. Paraffin-embedded brain tissues were sectioned into 5 μm slices, which were stained with HE. Images were acquired using 3DHISTECH slide scanners (DX12, Hungary).

2.2.7. Biochemical analysis

The brain tissues were homogenized in saline to form a 10 % (w/v) tissue homogenate, which was centrifuged at 3000 rpm for 10 min at 4 °C to obtain the supernatant. The levels of hydrogen peroxide (H_2O_2), nitric oxide (NO), malondialdehyde (MDA), superoxide dismutase (SOD), and glutathione (GSH) glutathione peroxidase (GSH-Px), total antioxidant capacity (T-AOC), catalase (CAT), lactate (LD), lactate dehydrogenase (LDH), succinate dehydrogenase (SDH), hexokinase (HK), pyruvate kinase (PK), Adenosine triphosphate (ATP), Ca^{2+}-Mg^{2+}-ATPase, and Na^{+}-K^{+}-ATPase in supernatant were determined using corresponding kits (Nanjing Jiancheng Bioengineering Institute, Nanjing, China) as per the manufacturer's protocol.

2.2.8. Measurement of inflammatory cytokines in serum and brain tissue

Blood was gathered by removing the eyeballs then centrifuged at 3000 rpm for 20 min at 4 °C for serum separation. The levels of inflammatory cytokines, including tumor necrosis factor-α (TNF-α), interleukin-6 (IL-6), and interleukin-10 (IL-10), in serum and brain tissue were assessed using the commercial ELISA kits (Jianglai Biotechnology Co., Ltd, Shanghai, China) as per the manufacturer's protocol.

2.2.9. Measurement of the activities of caspase-3 and -9 in brain tissue

The activities of caspase-3 and -9, as markers of apoptosis in brain tissue was assessed using commercial kits (Nanjing Jiancheng Bioengineering Institute, Nanjing, China) as per the manufacturer's protocol.

2.2.10. Terminal deoxynucleotidyl transferase-mediated dUTP nick-end labeling (TUNEL) staining

TUNEL staining was applied to identify apoptotic cells on paraffin sections (4 μm). Images was captured through fluorescence microscope. Green light presented the TUNEL-positive cells.

2.2.11. Western blot

The brain tissues were homogenized in lysis buffer on ice. Supernatant was collected after centrifugation at 12 000 rpm for 10 min. Protein concentration was assessed using a BCA assay kit (Solarbio Science & Technology Co., Ltd, Beijing, China). Then protein was separated by SDS-PAGE (Solarbio Science & Technology Co., Ltd, Beijing, China), and then transferred to the PVDF membranes (Millipore, USA). Membranes were blocked in PBST (phosphate-buffered saline with 0.1 % Tween 20) containing 5 % non-fat-dried milk at room temperature (RT) for 120 min and then incubated with primary antibodies against NF-κB p65 (1:1000), p-NF-κB p65 (1:1000), Myd88 (1:800), IκB-α (1:800), p-IκB-α (1:800), IL-6 (1:800), TNF-α (1:1000), NLRP3 (1:1000), Nrf2 (1:1000), HO-1 (1:1000), Bax (1:1000), Bcl-2 (1:1000), Cleaved Caspase-3 (1:1000), Claudin-1 (1:1000), MMP-9 (1:1000), Occludin (1:1000) and VEGF (1:1000) overnight at 4 °C. After washing four times with 1 × TBST (Tris Buffered Saline with Tween 20) for 10 min, the membranes were incubated with secondary antibodies at RT for 2 h with gentle shaking. The bands were visualized using ultrahigh sensitivity ECL chemiluminescent solution, and captured by ChemiDoc-It2 610 imaging system (UVP, LLC, Upland, CA, USA). Image J was used to quantify the band intensities and β-actin was used as a control.

2.2.12. Statistical analysis

The data were expressed as mean ± SEM or percent (%). Statistical analysis was performed using GraphPad Prism 8. Student's t-test or one-way ANOVA followed by Duncan's tests were used to compare the differences between groups. Mortality rates were compared using Fisher's exact test and Chi-square test. $p < 0.05$ was considered as statistical significance.

3. Results

3.1. Identification of potential targets of 6-OHG in treating HHBI

To investigate the potential targets of 6-OHG against HHBI, network pharmacology approach was employed. 566 potential action targets of 6-OHG were collected from the TCMSP, PharmMapper, SEA, superPred, and SWP databases. After integrating UniProt database entries and removing duplicates, 492 targets were obtained. Then, 1839 HHBI-related targets were collected from the GeneCards and OMIM databases. The intersection of 6-OHG and HHBI targets was shown as a Venn diagram (Fig. 1B). 186 intersection targets of 6-OHG in treating HHBI were obtained and used as the core targets for subsequent research.

3.2. PPI network analysis

We constructed the PPI network diagram by importing 186 intersection targets into the STRING database. Then the interaction relationships were further analyzed via importing the STRING data file into Cytoscape 3.7.2. As shown in Fig. 1C and D, there were 186

Table 1
GO terms in 6-OHG.

Term	Category	Name	Count	PValue
GO:0001666	BP	response to hypoxia	26	5.80E-22
GO:0043066	BP	negative regulation of apoptotic process	30	2.18E-14
GO:0006954	BP	inflammatory response	23	6.81E-11
GO:0046777	BP	protein autophosphorylation	16	2.21E-10
GO:0006468	BP	protein phosphorylation	23	2.82E-09
GO:0006508	BP	proteolysis	19	8.21E-08
GO:0090398	BP	cellular senescence	8	7.87E-07
GO:0071456	BP	cellular response to hypoxia	11	9.75E-07
GO:0050728	BP	negative regulation of inflammatory response	10	4.18E-06
GO:0097190	BP	apoptotic signaling pathway	7	8.81E-05
GO:0045121	CC	membrane raft	19	1.47647E-11
GO:0009986	CC	cell surface	28	2.49448E-11
GO:0005901	CC	caveola	12	9.68984E-11
GO:0043025	CC	neuronal cell body	20	5.67013E-09
GO:0048471	CC	perinuclear region of cytoplasm	27	5.99743E-09
GO:0005739	CC	mitochondrion	35	2.0294E-07
GO:0098978	CC	glutamatergic synapse	17	3.01722E-07
GO:0032991	CC	macromolecular complex	23	4.2072E-07
GO:0016324	CC	apical plasma membrane	16	1.65978E-06
GO:0016323	CC	basolateral plasma membrane	13	1.83419E-06
GO:0004713	MF	protein tyrosine kinase activity	16	3.43E-13
GO:0005102	MF	receptor binding	25	1.13E-12
GO:0008270	MF	zinc ion binding	32	4.81E-10
GO:0019901	MF	protein kinase binding	22	3.308E-08
GO:0020037	MF	heme binding	12	2.82449E-07
GO:0019903	MF	protein phosphatase binding	10	3.3483E-07
GO:0051117	MF	ATPase binding	8	3.68981E-05
GO:0016491	MF	oxidoreductase activity	11	0.000140834
GO:0008134	MF	transcription factor binding	10	0.000231276

nodes and 456 edges in the interaction network. The node degree average was 4.9, with 62 targets exceeding the average. The representative degree value was gradually reduced from deep to shallow. Nodes with the degree top 5 were: SRC, PIK3R1, HSP90AA1, AKT1 and HRAS.

3.3. GO term and KEGG pathway enrichment analysis

To fully clarify the potential mechanism of 6-OHG against HHBI, we performed GO and KEGG enrichment analysis of the targets in the PPI network using DAVID 6.8. As shown in Fig. 1E and Table 1, GO analysis indicated that targets were significantly enriched in the following terms. BP was mainly involved in response to hypoxia, inflammatory response, and cellular senescence, CC was mainly involved in membrane rafts, mitochondria, and neuronal cytosol, and MF was mainly involved in receptor binding, heme binding, and oxidoreductase activity. KEGG enrichment analysis indicated that core targets were mainly enriched in the NF-κB signaling pathway, TNF signaling pathway, HIF-1 signaling pathway, and VEGF signaling pathway (Fig. 1F). Both GO and KEGG enrichment analysis indicated that the therapeutic effect of 6-OHG on HHBI was mostly related to the regulation of oxidative stress injury and inflammatory response. Then, the above mechanisms will be verified in the subsequent experiments *in vivo*.

3.4. 6-OHG prolonged the survival time of mice in the normobaric hypoxia test

Normobaric hypoxia animal model was used for evaluating the anti-hypoxic activity of 6-OHG. As presented in Table 2, compared with the model group, the survival time of mice under hypoxia environment in all dose 6-OHG groups were remarkably extended ($p < 0.01$ or $p < 0.05$). The prolongation rates were 21.97 %, 31.16 % and 41.41 % in the low, medium and high dose 6-OHG treated groups, respectively.

3.5. 6-OHG decreased the mortality rate of mice in the acute decompression hypoxia test

Acute decompression hypoxia test was employed for evaluating the HH tolerance effect of 6-OHG. As illustrated in Table 3, the mortality rate of mice under acute decompression hypoxia exposure was reduced from 100 % to 60 % after acetazolamide intervention. Treatment with 6-OHG at doses of 25, 50 and 100 mg/kg reduced the mortality rates of mice under acute decompression hypoxia environment to 80 %, 70 %, and 50 %, respectively. Lower mortality rate and longer survival time represented better protection against injury induced by hypoxia. Considering high dose of 6-OHG exhibited the best protective effect for hypoxia mice, the subsequent experiments were performed at dose of 100 mg/kg.

3.6. 6-OHG reduced neuronal damage in the brain of mice exposed to HH

HE staining was used to explored whether 6-OHG treatment could improve neuronal damage and loss induced by HH. As illustrated in Fig. 2, the cortical cells in the control group were regularly arranged with clear boundaries and normal cell structure. Following HH exposure, the cortical cells showed lesions, irregular cell arrangement and disorder, nuclear fixation, reduced neuronal cell, and vascular edema. After the administration of 6-OHG, the cell damage in mice brain tissue was significantly improved as evidenced by the normalization of cell morphology, the reduction of cell swelling, and the improvement of cellular nucleus crumpling. In summary, 6-OHG alleviates the pathological damage of mice caused by HHBI.

3.7. 6-OHG attenuates HH induced oxidative stress in mice brain

One of the key factors in HH induced neuronal cell damage is oxidative stress [9]. To further verify the neuroprotective effect of 6-OHG in HH mice, we determined the oxidative stress markers. Compared to the control group, the biochemical analysis indicated that the levels of NO, H_2O_2 and MDA were remarkably elevated in the brain of mice exposed to HH ($p < 0.01$), while 6-OHG treatment remarkably decreased the contents of NO, H_2O_2 and MDA ($p < 0.05$; Fig. 3A–C). At the same time, the levels of SOD, GSH, CAT, GSH-Px, and T-AOC were remarkably decreased in the brain of mice exposed to HH ($p < 0.01$), while 6-OHG treatment significantly increased the levels of these factors ($p < 0.05$ or $p < 0.01$; Fig. 3D–H). All these results suggest that 6-OHG administration significantly

Table 2
| Effect of 6-OHG on the survival time of mice in normobaric hypoxia test (x ± s, n = 10).

Group	Dose (mg/kg)	Survival time (min)	Prolongation rate (%)
Hypoxia group	–	38.05 ± 4.91	–
Acetazolamide group	200	47.81 ± 4.63[b]	25.64
6-OHG group	25	46.41 ± 4.82[a]	21.97
	50	49.91 ± 5.09[b]	31.16
	100	53.81 ± 7.90[b]	41.41

Data are expressed as mean ± SEM or percent (%).
[a] $P < 0.05$.
[b] $P < 0.01$ vs. Hypoxia group.

Table 3
Effect of 6-OHG on the mortality of mice in acute decompression hypoxia test (x ± s, n = 10).

Group	Dose (mg/kg)	Number of deaths (single)	Mortality (%)
Acute decompression group	–	10	100
Acetazolamide group	200	6	60[b]
	25	8	80[a]
6-OHG group	50	7	70[b]
	100	5	50[b]

Data are expressed as percent (%).
[a] $P < 0.05$.
[b] $P < 0.01$ vs. Acute decompression group.

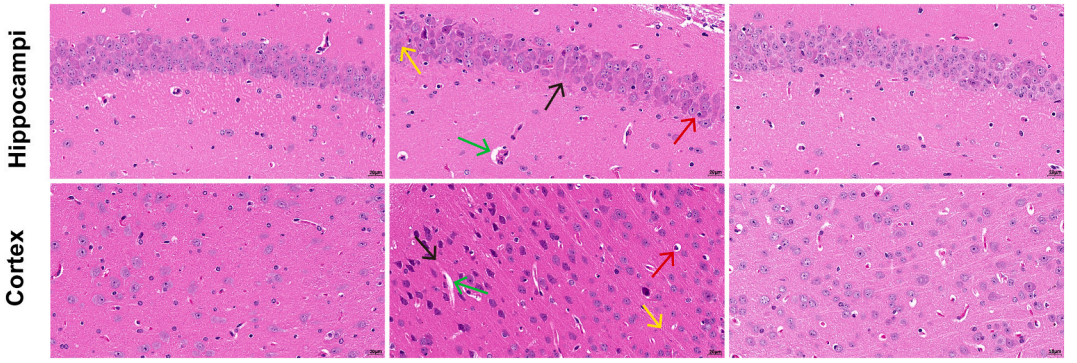

Fig. 2. Effects of 6-OHG on brain histopathological changes in mice with HHBI. The scale bar was 20 μm. The scanning magnification of 200 times. Black arrow: irregular cell arrangement and disorder. Red arrow: nuclear fixation. Yellow arrow: reduced neuronal cell. Green arrow: vascular edema. (For interpretation of the references to colour in this figure legend, the reader is referred to the Web version of this article.)

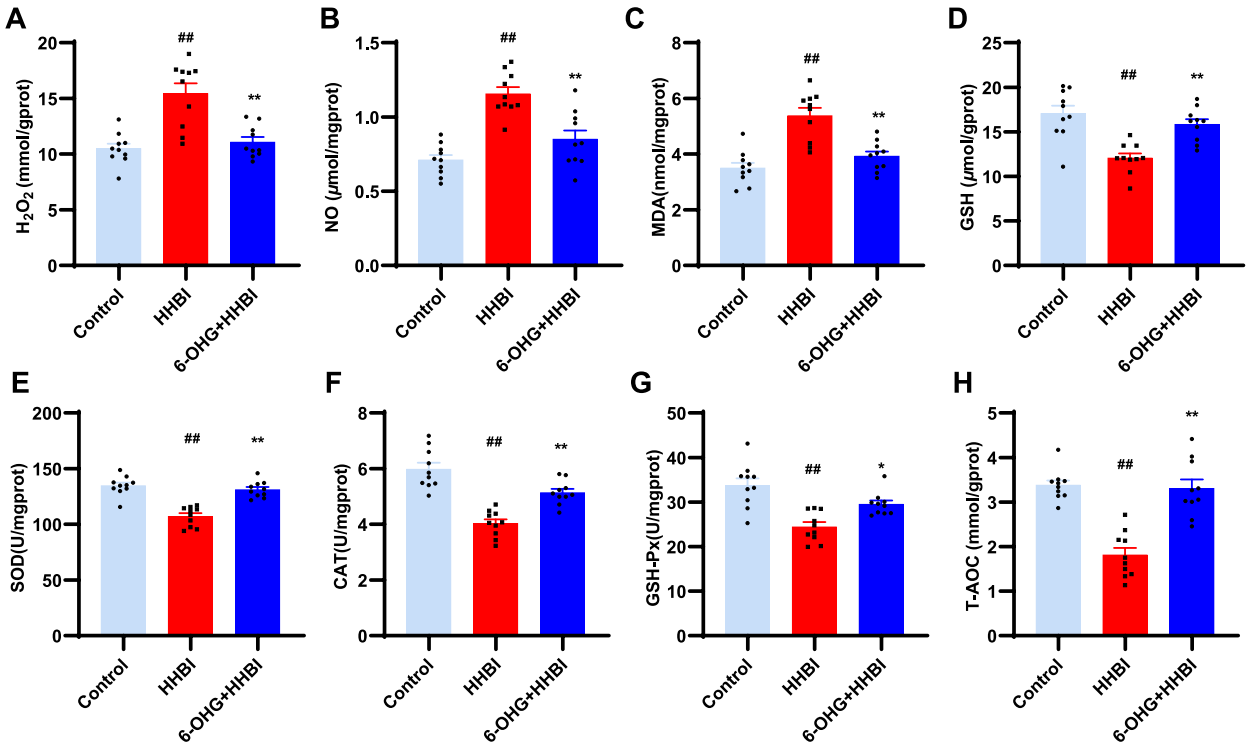

Fig. 3. Effects of 6-OHG on oxidative stress in brain tissue of mice with HHBI. The levels of H_2O_2 (A), NO (B) MDA (C), GSH (D), SOD (E), CAT (F), GSH-Px (G) and T-AOC (H) in brain tissues. Data (n = 10 per group) are represented as means ± SEM. $^{\#}p < 0.05$ and $^{\#\#}p < 0.01$ vs the control group; $^{*}p < 0.05$ and $^{**}p < 0.01$ vs the HHBI group.

attenuates oxidative stress induced by HH.

3.8. 6-OHG promotes HIF-1α destabilization in brain of mice exposed to HH

As shown in Fig. 4, HH exposure appreciably increased the expression of HIF-1α and its downstream gene VEGF as compared to normoxia control. 6-OHG administration significantly reduced the HIF-1α and VEGF protein expression levels compared to the HH groups.

3.9. 6-OHG attenuates HH-induced energy metabolism disorder in mice brain

To determine the role of 6-OHG in the regulation of energy metabolism, levels of SDH, PK, HK, ATP, Na^+-K^+-ATPase, Ca^{2+}-Mg^{2+}-ATPase, LDH and LD in brain tissue were measured. As illustrated in Fig. 5, HH exposure significantly decreased the levels of Na^+-K^+-ATPase, Ca^{2+}-Mg^{2+}-ATPase, SDH, PK, HK and ATP, remarkably increased the levels of LD and LDH, indicating that HH caused energy metabolism disorder. Nevertheless, 6-OHG administration significantly reversed these changes ($p < 0.05$ or $p < 0.01$). These results suggest that 6-OHG effectively mitigates the disruption of energy metabolism induced by HH.

3.10. 6-OHG suppressed HH induced apoptosis in mice brain

HHBI is often accompanied by cellular apoptosis [20]. TUNEL staining indicated that more apoptotic cells (green) were observed in the HH group compared to the normoxia group. However, 6-OHG treatment remarkably reduced the number of apoptotic cell compared to the HH group (Fig. 6A). In addition, HH exposure significantly increased the activities of caspase-3 and -9 ($p < 0.01$, Fig. 6B and C), while 6-OHG treatment significantly decreased their activities. To explore the mechanism of 6-OHG on HH induced apoptosis, we assessed the expressions of apoptosis related proteins in brain tissue, such as Bcl-2, Bax, and cleaved caspase-3 (Fig. 6D). The results suggested that HH stimulation significantly elevated the expressions of pro-apoptotic protein levels of Bax (Fig. 6E) and cleaved caspase-3 (Fig. 6F), while significantly reduced the expressions of anti-apoptotic protein Bcl-2 (Fig. 6G) and the ratio of Bcl-2/Bax (Fig. 6H) compared to the normoxia group. Nevertheless, 6-OHG treatment dramatically reversed these changes. These results indicate that 6-OHG protects the brain from HH induce apoptosis.

3.11. 6-OHG activates the Nrf2/HO-1 signaling pathways in brain of mice exposed to HH

The Nrf2/HO-1 signaling pathway is related to oxidative stress and inflammation response [21]. To elucidate the mechanisms by which 6-OHG regulates oxidative stress, the expressions of Nrf2 and HO-1 were detected. As illustrated in Fig. 7A–C, the protein levels of Nrf2 and HO-1 were elevated notably after HH stimulation and were further increased after 6-OHG treatment ($p < 0.05$ or $p < 0.01$). Furthermore, molecular docking was performed by AutoDock Vina to verify the potential binding of 6-OHG to Nrf2 and HO-1. As illustrated in Fig. 7D and E, amino acid residues Ser555, Ser508, Arg415 and Arg483 of the Nrf2 protein and amino acid residues Gln38 and Arg136 of the HO-1 protein formed hydrogen bond with 6-OHG. The affinities of 6-OHG with Nrf2 and HO-1 were −6.4 and −7.7 kcal/mol, respectively, which indicated that 6-OHG might be stably bound to Nrf2 and HO-1. These results suggest that 6-OHG treatment activates the Nrf2/HO-1 pathway against HHBI.

3.12. 6-OHG attenuates HH induced inflammatory response in mice brain

HH induced neuroinflammation is another critical factor of brain injury [22]. To evaluate the *anti*-neuroinflammatory activity of

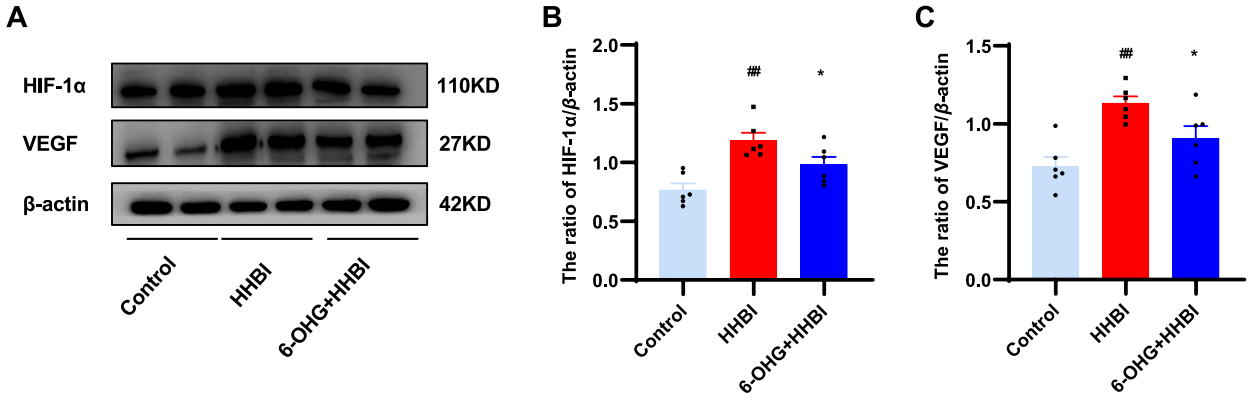

Fig. 4. Effects of 6-OHG on HIF-1α and VEGF in brain tissue of mice with HHBI. (A) Western blotting analysis of HIF-1α and VEGF proteins expression (The original image is provided in the Supplementary Fig. S1). Quantification analysis of HIF-1α (B) and VEGF (C). Data (n = 6 per group) are represented as means ± SEM. $^{\#}p < 0.05$ and $^{\#\#}p < 0.01$ vs the control group; $^{*}p < 0.05$ and $^{**}p < 0.01$ vs the HHBI group.

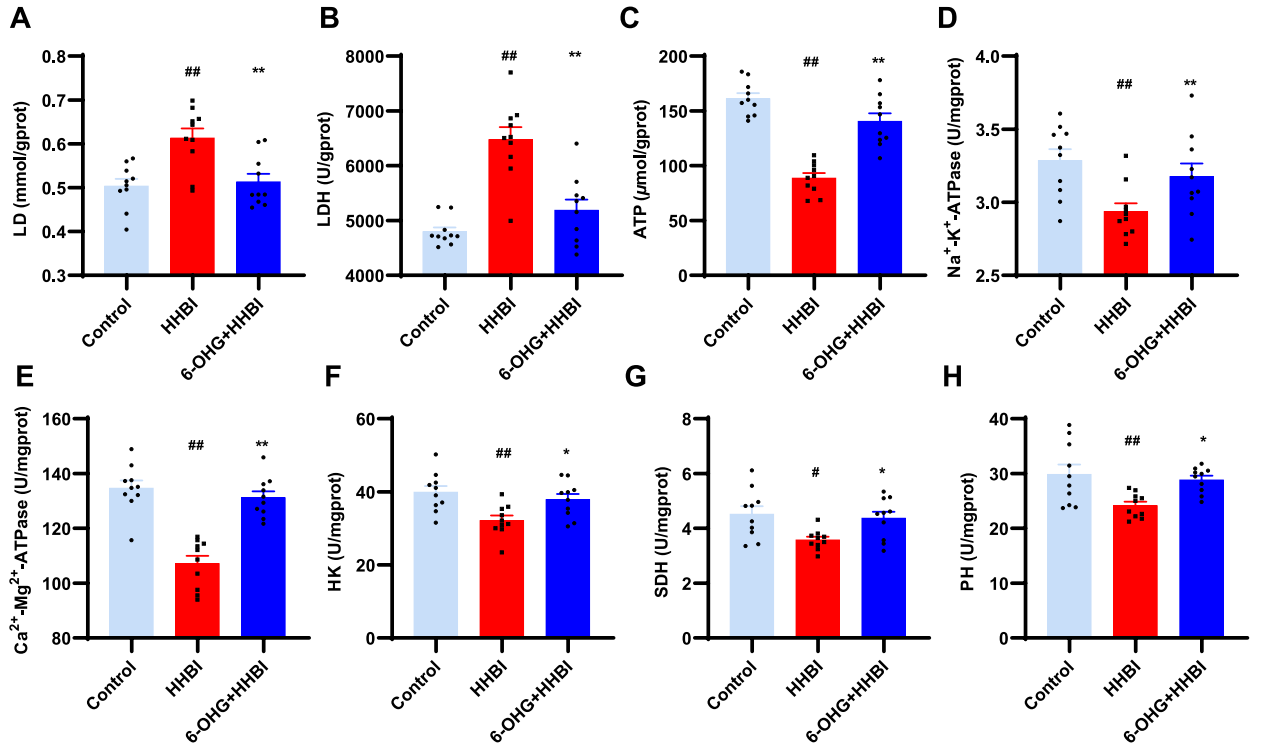

Fig. 5. Effects of 6-OHG on energy metabolism in brain tissue of mice with HHBI. The levels of H_2O_2 (A), NO (B) MDA (C), GSH (D), SOD (E), CAT (F), GSH-Px (G) and T-AOC (H) in brain tissues. Data (n = 10 per group) are represented as means ± SEM. $^{\#}p < 0.05$ and $^{\#\#}p < 0.01$ vs the control group; $^{*}p < 0.05$ and $^{**}p < 0.01$ vs the HHBI group.

6-OHG, we measured the two pro-inflammatory cytokines IL-6, TNF-α, and an anti-inflammatory cytokine IL-10 by ELISA. Our results demonstrated that HH exposure significantly increased the levels of IL-6 and TNF-α and reduced the content of IL-10 in serum and brain tissues of mice, while 6-OHG treatment remarkably reversed these changes ($p < 0.05$, Fig. 8A–F). These findings suggest that 6-OHG inhibits the inflammatory response and may represent an effective treatment for HHBI.

3.13. 6-OHG improved HH induced blood brain barrier (BBB) injury in mice

It has been demonstrated that HH induces disruption of BBB [23]. To explore the protective effect of 6-OHG against HH induced BBB injury, we determined the expressions of BBB-related proteins, including MMP-9, Claudin-1, and Occludin by western blotting. As illustrated in Fig. 9, HH exposure significantly resulted in the downregulation of Occludin and Claudin-1, and the upregulation of MMP-9 in brain tissue ($p < 0.05$ or $p < 0.01$). Nevertheless, the tendency was reversed by 6-OHG treatment, indicating the protective roles of 6-OHG against HH induced BBB dysfunction.

3.14. 6-OHG inhibited the NF-κB/NLRP3 signaling pathways in brain of mice exposed to HH

It has been noted that HH exposure promotes the release of various pro-inflammatory factors through activation of the NF-κB/NLRP3 pathway [24]. To further investigate whether the anti-inflammatory action of 6-OHG was related to the inhibition of the NF-κB/NLRP3 signaling pathway, we tested the expression of several key proteins. As illustrated in Fig. 10A–G, HH stimulation upregulated the protein expression of p-NF-κB p65, NLRP3, p-IκB-α, MyD88, IL-6, and TNF-α in the brain tissue of mice, while 6-OHG treatment reversed these changes ($p < 0.05$ or $p < 0.01$). Molecular docking results revealed that amino acid residues Arg73 and Asn139 of the NF-κB protein and amino acid residues Ile521 and Thr169 of the NLRP3 protein formed hydrogen bond with 6-OHG. The affinities of 6-OHG with NF-κB and NLRP3 were −6.7 and −8.5 kcal/mol, respectively, suggesting that 6-OHG might be stably bound to these proteins (Fig. 10H and I). These findings indicate that 6-OHG alleviates HH induced inflammatory response by suppressing the NF-κB/NLRP3 signaling pathways.

4. Discussion

High altitude environment is characterized by low pressure and low oxygen, which is the most critical factor affecting human health [3]. The brain is susceptible to alterations in O_2 supply. Thus, human exposure to high altitudes can cause irreversible damage to

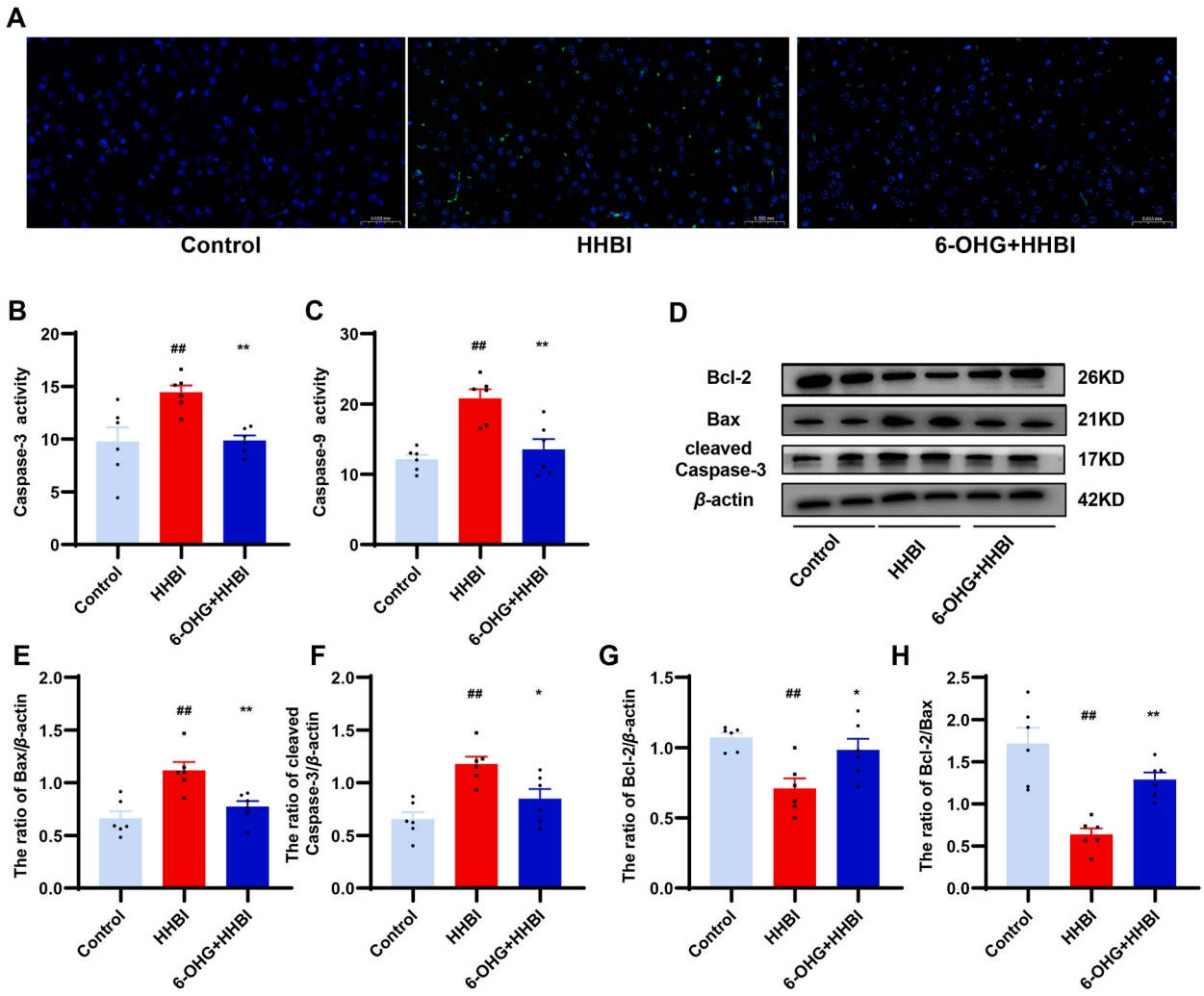

Fig. 6. Effects of 6-OHG on apoptotic in brain tissue of mice with HHBI. (A) TUNEL staining. The activities of caspase-3 (B) and caspase-9 (C). (D) Western blotting analysis of Bax, Bcl-2 and cleaved caspase-3 proteins expression (The original image is provided in the Supplementary Fig. S2). Quantification analysis of Bax (E), Bcl-2 (F), Bax/Bcl-2 (G) and cleaved caspase-3 (H). Data (n = 3/6 per group) are represented as means ± SEM. $^{\#}p < 0.05$ and $^{\#\#}p < 0.01$ vs the control group; $^{*}p < 0.05$ and $^{**}p < 0.01$ vs the HHBI group.

brain. In our study, the beneficial effects of 6-OHG on HHBI and its underling mechanisms were explored by integrated network pharmacology and mice model of HHBI. We found that 6-OHG treatment attenuated oxidative stress and inflammation response, prevented energy disorder and apoptosis as well as maintained the BBB integrity in HHBI mice. In addition, 6-OHG administration elevated the expression of Nrf2 and its downstream HO-1, reduced the expression of NF-κB and NLRP3 and thereby inhibiting oxidative stress and inflammation response. Hence, our results manifest that 6-OHG can be effective against HHBI by stimulating the Nrf2/HO-1 signaling pathway and suppressing the NF-κB/NLRP3 signaling pathway.

In this study, we first verified the anti-hypoxia activities and optimal dose of 6-OHG using normobaric hypoxia test and acute decompression hypoxia tolerance test. The results indicated that 6-OHG treatment significantly increased the survive time of mice under hypoxic condition and reduced the mortality rate of mice under acute decompression hypoxia stimulation, exhibited excellent anti-hypoxia activity. Notably, 6-OHG showed best protective activity at the dose of 100 mg/kg. Studies have shown that HH induces the pathological damage of neurons in the brain [8,20]. Consistent with the previous studies, the results of HE staining in this study also indicated that the neurons of cortex region underwent pathological damage in HH mice. 6-OHG treatment ameliorated the cortical neuronal damage, suggesting that 6-OHG exhibited protective effect on HHBI.

HHBI is a complex pathophysiological process with various mechanisms [25]. Flavonoids also exert beneficial effects via a number of different mechanisms [26]. Network pharmacology is an emerging interdisciplinary discipline based on systems biology, genomics, proteomics and other disciplines, which integrates a large amount of information by combining computational analyses with *in vivo* and *in vitro* experiments, and predicts the potential targets and mechanisms of action of natural compounds from a systemic perspective [18]. Therefore, in the current study, we utilized network pharmacology to investigate the potential therapeutic targets and molecular

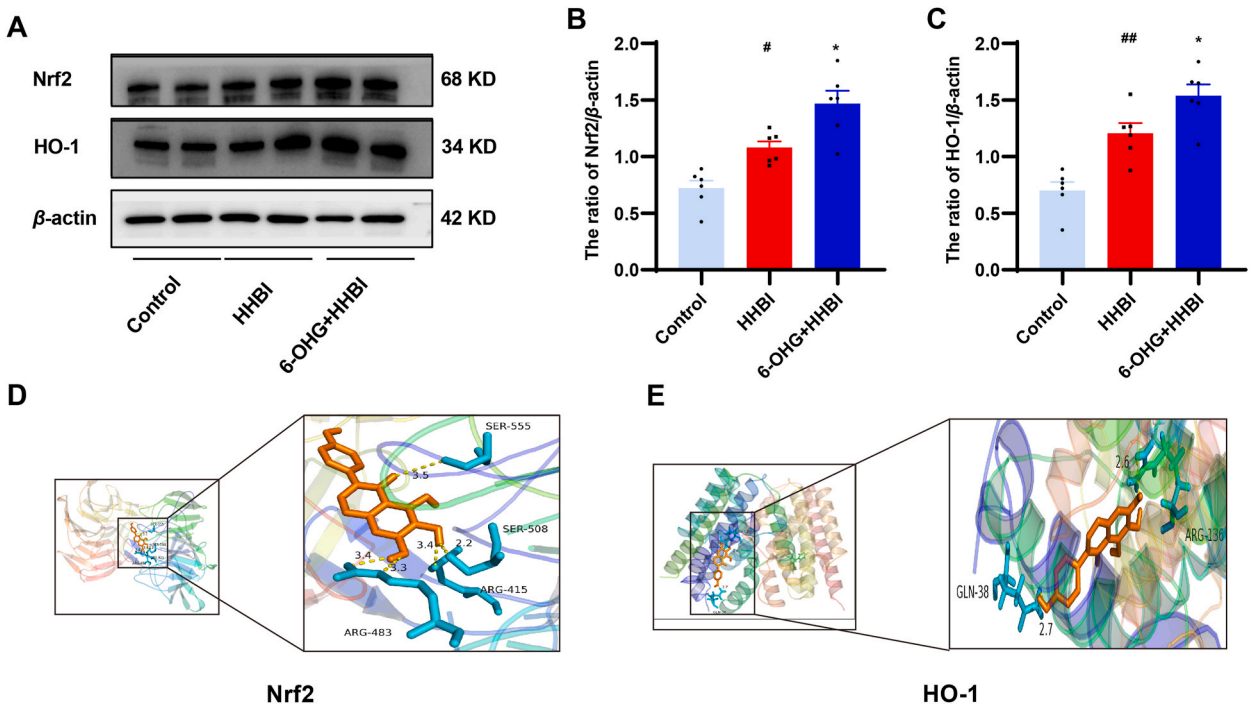

Fig. 7. Effects of 6-OHG on Nrf2/HO-1 signaling pathway in brain tissue of mice with HHBI. (A) Western blotting analysis of Nrf2 and HO-1 proteins expression (The original image is provided in the Supplementary Fig. S3). Quantification analysis of Nrf2 (B) and HO-1 (C). Data (n = 6 per group) are represented as means ± SEM. $^{\#}p < 0.05$ and $^{\#\#}p < 0.01$ vs the control group; $^{*}p < 0.05$ and $^{**}p < 0.01$ vs the HHBI group. Molecular docking of 6-OHG binding to the Nrf2 (E) and HO-1 (F).

mechanisms of 6-OHG against HHBI. Network pharmacology analysis indicated the targets of 6-OHG against HHBI were mainly enriched in oxidative stress, apoptotic, HIF-1 signaling pathway, NF-κB signaling pathway and TNF signaling pathway, which suggested that oxidative stress, inflammation and apoptotic might be the potential mechanisms associated with the protective effects of 6-OHG against HHBI.

Under HH environments, reduced oxygen availability may impair mitochondrial respiration and suppress the enzymatic antioxidant system, leading to excessive production of free radical, then result in oxidative stress [7]. H_2O_2 and NO are two primary form of oxygen-derived reactive oxygen species [27]. MDA is a product of the lipid peroxidationa and reflects the degree of cell membrane system damage [28]. SOD, GSH-Px and CAT are essential endogenous antioxidant enzymes that maintain intracellular redox homeostasis by eliminating ROS [29]. GSH is an obligate co-substrate of GSH-Px for the reduction of H_2O_2 to H_2O [30]. T-AOC reflects the ROS scavenging ability of the body. In this study, we found that HH exposure caused oxidative stress response in mice brain as shown by raised levels of H_2O_2, NO, and MDA and decreased levels of GSH, SOD, CAT, GSH-Px, and T-AOC. 6-OHG treatment decreased the H_2O_2, NO, and MDA concentrations along with increased the antioxidant enzymes activities in the brain of mice under HH condition, indicating that oxidative stress induced by HH was mitigated.

HIF-1α is one of the predominant transcription factor under hypoxia conditions and acts as a key regulator of oxygen homeostasis [31]. Apart from hypoxia, HIF-1α is also induced by ROS [32]. Activation of HIF-1α can exert protective role, but overexpression of HIF-1α may also contribute to cell and tissue damage [33]. Thus, HIF-1α can be regarded as both hypoxia stress and pro-oxidant indicator. VEGF is a key downstream effector of HIF-1α, which binds specifically with vascular endothelial cells, leading to endothelial cell growth, and thus promoting neovascularization [34]. However, increased expression of VEGF also impaired endothelial barrier integrity, enhances vascular permeability, and induces brain injury [35] and even HACE [36]. Accumulating evidence have indicated that HH exposure promotes the expression of HIF-1α and VEGF [37,38]. Consistent with the previous results, we also found that HH stimulation significantly enhanced the levels of HIF-1α and VEGF, while treatment of 6-OHG reduced the expressions of HIF-1α and VEGF, suggesting that 6-OHG could promote HIF-1α destabilization via suppressing ROS level and hypoxia stress induced by HH.

Mitochondria is main organelle responsible for energy production and also the major source involved in ROS production [39]. Overgenenated ROS induced by HH are able to attack mitochondria, leading to an imbalance in energy metabolism [40]. Previous studies have revealed that HH could induce the distinct expression of proteins and genes associations with energy metabolism in brain [41] and hippocampal tissue [42]. In addition, Jiang et al. revealed that HH stimulation led to decrease in the levels of ATP, ATPase, SDH, PK, and HK in brain tissue and increase in the levels of LD and LDH in serum [24]. Recently, Meng et al. also indicated that energy metabolism dysfunction was one of the main cause of HHBI [43]. With consistent these previous studies, we observed an decrease in the ATP content and the activities of ATPases and glycolysis enzymes (SDH, HK and PK), but a increase in the levels of LD and LDH in

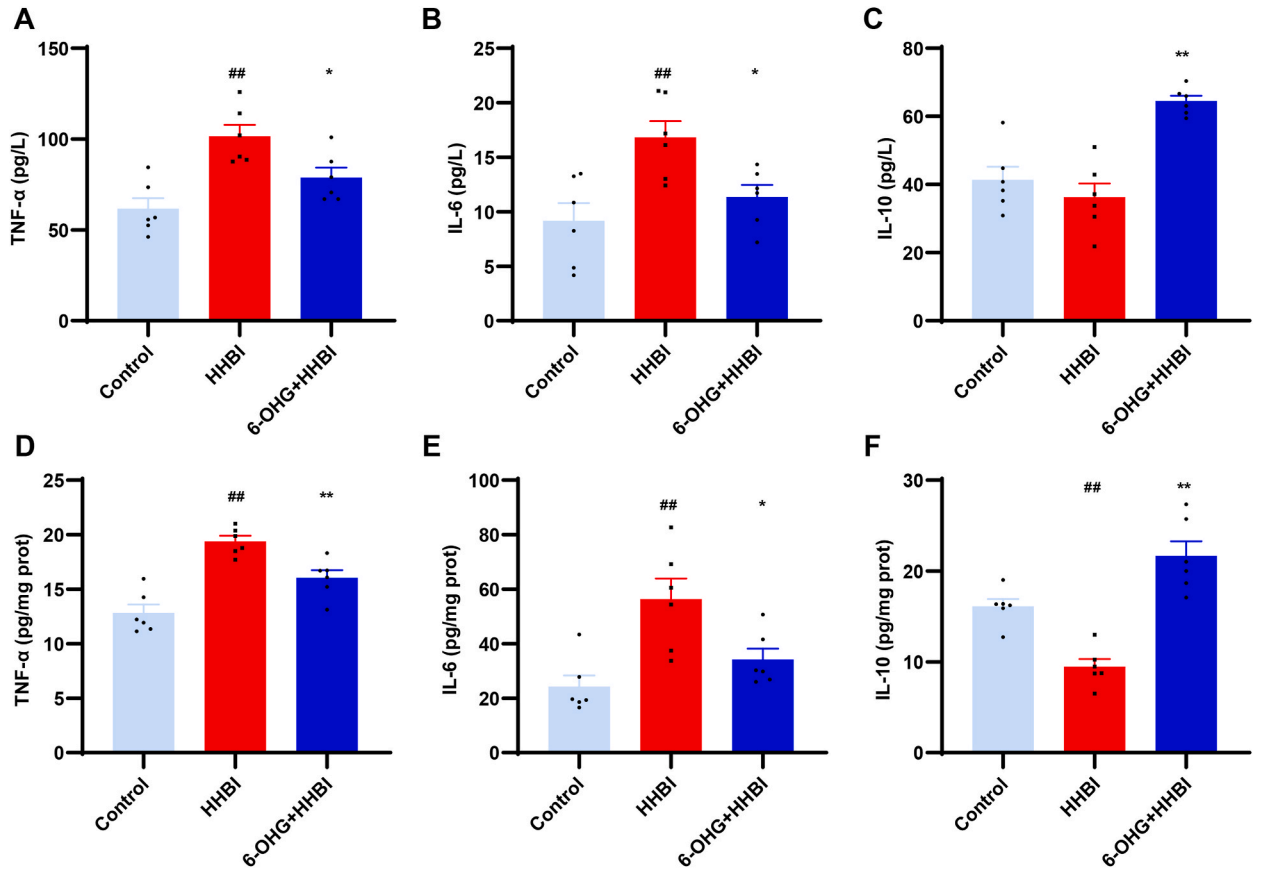

Fig. 8. Effects of 6-OHG on inflammatory response in HHBI mice. The levels of TNF-α (A and D), IL-1β (B and E) and IL-8 (C and F) in serum and brain tissues. Data (n = 6 per group) are represented as means ± SEM. $^{\#}p < 0.05$ and $^{\#\#}p < 0.01$ vs the control group; $^{*}p < 0.05$ and $^{**}p < 0.01$ vs the HHBI group.

brain tissue of mice with HHBI, while 6-OHG treatment reversed these changes, mitigating HH induced dysfunction of energy metabolism.

Excessive ROS caused by HH can result in neuronal apoptosis, which also plays a vital role in pathogenesis of HHBI [44] and has received increasing attention in recent years. Comfortably, our findings indicated that HH resulted in more apoptosis cell in the mice brain analyzed by TUNEL assay, whereas 6-OHG treatment effectively mitigated the cell apoptosis induced by HH. Caspase-9 and -3 act as initiator caspases and executioner caspases, respectively, and play a vital role in the mitochondria-dependent intrinsic apoptosis pathway [45]. The Bcl-2 family of proteins is the critical regulator of mitochondrial apoptosis, and can be categorized into promoters of cell death, such as Bcl-2 and Bcl and inhibitors of cell death, including Bax and Bak [46]. Our results revealed that the activities of caspase −3 and −9, and the expressions of Bax and cleaved caspase-3 were notably increased, while the level of Bcl-2 was significant reduced in the brain of mice after HH stimulation. 6-OHG treatment reversed these change. All these results support the anti-apoptosis capacity of 6-OHG in response to HHBI.

Nrf2 is an important intracellular regulator associated with oxidative stress [47]. Upon activation, Nrf2 translocates to the nucleus and binds to the antioxidant response elements (ARE), thereby triggering the transcription of numerous downstream molecules such as HO-1 [48]. HO-1 is an antioxidative enzyme responsible for several antioxidant, anti-inflammatory, and anti-apoptotic pathways. Activation of the Nrf2/HO-1 signaling pathway has been reported to be effective in preventing HH induced damage, including acute mountain sickness (AMS) [49], HAPE [50], high altitude pulmonary edema (HAPE) [51], high altitude pulmonary hypertension [52] and high altitude heart injury [53]. Our findings indicated that HH stimulation enhanced the expressions of Nrf2 and HO-1 in mice brain, that may be considered as a compensatory mechanism to mitigate HH induced injury. 6-OHG treatment further enhanced the expressions of Nrf2 and HO-1 in HH mice brain, indicating that antioxidant and anti-apoptosis properties of 6-OHG may be achieved partly by activation of Nrf2/HO-1 signaling pathway.

There is a general consensus that oxidative stress caused by HH lead to elevation of pro-inflammatory cytokines that may contribute to HHBI [54]. Clinical studies have proved that pro-inflammatory cytokines are elevated in individuals acutely exposed to high altitude [55,56]. Another clinical study also has shown individuals who experience AMS have higher levels of pro-inflammatory cytokines in serum compared with those who do not [57]. Experimental animal studies also indicate that HH promotes the release of pro-inflammatory cytokines, including TNF-α, IL-6, and IL-1β in serum and brain of mice [58]. In agreement with previous studies, we

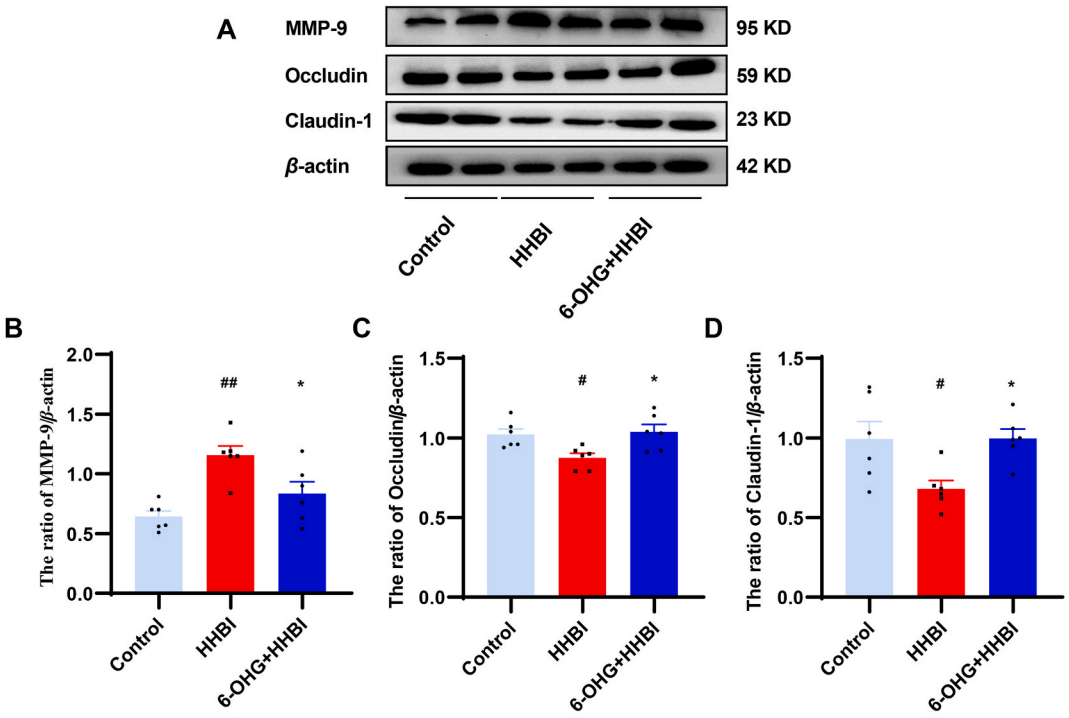

Fig. 9. Effects of 6-OHG on blood brain barrier (BBB) injury in brain tissue of mice with HHBI. (A) Western blotting analysis of MMP-9, Claudin-1, and Occludin proteins expression (The original image is provided in the Supplementary Fig. S4). Quantification analysis of MMP-9 (B), Occluding (C), and Claudin-1(D). Data (n = 6 per group) are represented as means ± SEM. $^{\#}p < 0.05$ and $^{\#\#}p < 0.01$ vs the control group; $^{*}p < 0.05$ and $^{**}p < 0.01$ vs the HHBI group.

also found that HH stimulation increased the levels of IL-6 and TNF-α, and decrease the content of anti-inflammatory cytokine IL-10 in serum and brain of mice. These effects were immensely reversed by administration of 6-OHG.

HH triggers the release of inflammatory and angiogenic mediators, thereby disrupting the BBB and promoting vasogenic edema [54]. Therefore, BBB disruption, characterized by structural breakdown of tight junction (TJ) protein, is a major pathological change after HH exposure and contribute to HHBI [37]. Maintenance of BBB integrity may be an effective pathway for drugs to exert protective effect against HHBI [59]. Occludin and claudin-5 are the two major TJ proteins for maintaining the function of the BBB [60]. MMP-9 is a zinc-dependent protease, can trigger the dysfunction of the BBB by degrading extracellular matrix and TJ proteins [61]. Recent studies have confirmed that HH exposure significantly down-regulated the expressions of occludin and claudin-5, inducing BBB disruption [8,24]. Comfortably, we also observed that the expressions of claudin 5 and occludin were downregulated, and the expression of MMP-9 was elevated in brain tissues of mice exposed to HH. Whereas 6-OHG treatment reversed these effects and ameliorated the disruption of BBB caused by HH.

NF-κB is a key transcription factor participating in inflammatory response [62]. Under normal conditions, NF-κB is inactive and sequestered in the cytoplasm by IkappaB protein (IκB, inhibitors of NF-κB). In reaction to inflammation, IκB kinase (IKK) degrades IκB proteins in the cytoplasm and release NF-κB from IκBα, and then NF-κB translocates from the cytoplasm to the nucleus to stimulate the generation of pro-inflammator cytokines, including TNF-α, IL-1β, and IL-6 [63]. Moreover, NF-κB is also a key mediator of the initiation signals required for the activation of NLRP3 inflammasome, which is multiprotein complex composed of NLRP3, pro-cysteinyl aspartate specific proteinase-1 (pro-caspase-1) and apoptosis-associated speck-like protein CARD domain (ASC) [64]. Activation of the NLRP3 inflammasome led to caspase-1 cleaved into its active form (IL-1β and IL-18), which in turn enhances inflammatory response [65]. Moreover, NLRP3 inflammasome can impairs the integrity of BBB. Recent research reported that NF-κB/NLRP3 signaling pathway was activated under HH condition and inhibiting the activation of NF-κB/NLRP3 signaling pathway could alleviate HHBI [8,24]. Similarly, our results showed that HH significantly triggered upregulations of NF-κB/NLRP3 signaling pathway-related proteins, including p-NF-κB, NLRP3, p-IκB-α, MyD88, IL-6, and TNF-α. In contrast, 6-OHG treatment markedly reversed these alterations, suggesting that 6-OHG exhibits anti-inflammatory property via downregulating NF-κB/NLRP3 signaling pathways.

Taken together, this study firstly reveals the protective effects of 6-OHG against HHBI in mice. The underling mechanism may be associated with the suppression of oxidative stress, inflammation, energy disorder, BBB disruption and apoptosis, via activation of the Nrf2/HO-1 singling pathways and inactivation of the NF-κB/NLRP3 singling pathways. These preliminary results suggest that 6-OHG can be developed as prophylactic and therapeutic candidate for HHBI. In future research, agonists or inhibitors of Nrf2/HO-1 and NF-κB/NLRP3 singling pathways will be applied to further verify the precise mechanisms of 6-OHG against HHBI.

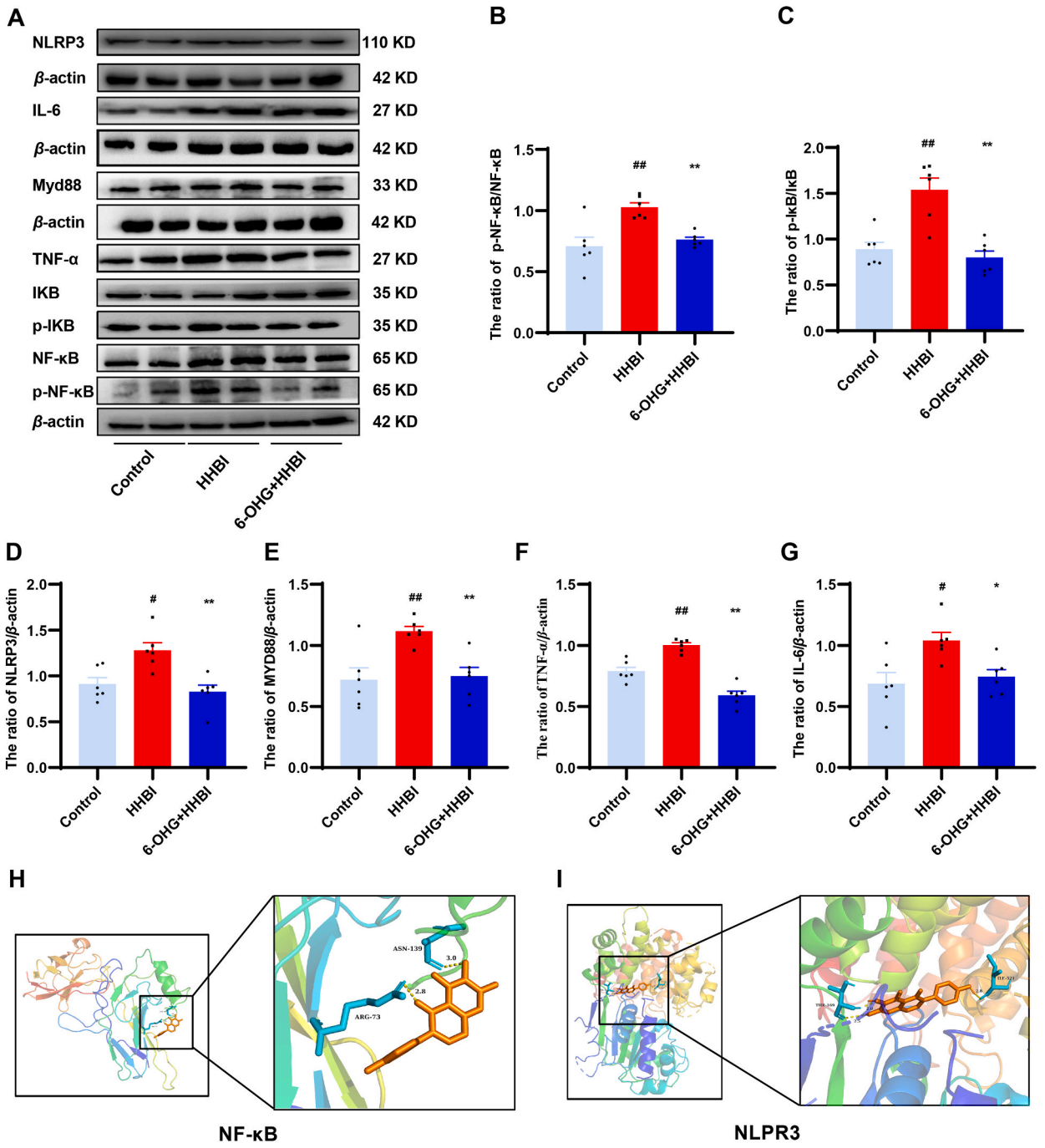

Fig. 10. Effects of 6-OHG on NF-κB/NLRP3 signaling pathway in brain tissue of mice with HHBI. (A) Western blotting analysis of NF-κB, p-NF-κB, NLRP3, IκB-α, p-IκB-α, MyD88, IL-6, and TNF-α proteins expression (The original image is provided in the Supplementary Figs. S4 and S5). Quantification analysis of p-NF-κB/NF-κB (B), p-IκB-α/IκB-α (C), NLRP3 (D), MyD88 (E), IL-6 (F), and TNF-α (G). Data (n = 6 per group) are represented as means ± SEM. $^{\#}p < 0.05$ and $^{\#\#}p < 0.01$ vs the control group; $^{*}p < 0.05$ and $^{**}p < 0.01$ vs the HHBI group. Molecular docking of 6-OHG binding to the NF-κB (H) and NLRP3 (I).

Funding

This work was supported by the National Natural Science Foundation of China (81872796), Natural Science Foundation of Gansu Province (22JR11RA011) and Institutional Foundation of The First Affiliated Hospital of Xi'an Jiaotong University (2022MS-11).

Ethics declarations

This study was reviewed and approved by Animal Care and Use Committee of 940th Hospital with the approval number: [2021KYLL241], dated [November 06, 2021].

Data availability statement

Data included in article/supp. material/referenced in article.

CRediT authorship contribution statement

Zhiqun Shi: Writing – original draft, Methodology, Investigation, Formal analysis, Data curation, Conceptualization. **Jie Zhang:** Writing – original draft, Investigation, Formal analysis, Data curation. **Huiping Ma:** Writing – review & editing, Supervision, Project administration, Funding acquisition. **Linlin Jing:** Writing – review & editing, Supervision, Resources, Project administration, Funding acquisition, Conceptualization.

Declaration of competing interest

The authors declare that they have no known competing financial interests or personal relationships that could have appeared to influence the work reported in this paper.

Appendix A. Supplementary data

Supplementary data to this article can be found online at https://doi.org/10.1016/j.heliyon.2024.e36241.

References

[1] G.S. Hao, Q.L. Fan, Q.Z. Hu, Q. Hou, Research progress on the mechanism of cerebral blood flow regulation in hypoxia environment at plateau, Bioengineered 13 (2022) 6353–6358, https://doi.org/10.1080/21655979.2021.2024950.
[2] P. Bärtsch, E.R. Swenson, Clinical practice: acute high-altitude illnesses, N. Engl. J. Med. 368 (2013) 2294–2302, https://doi.org/10.1056/NEJMcp1214870.
[3] Y. Li, Y. Zhang, Y. Zhang, Research advances in pathogenesis and prophylactic measures of acute high altitude illness, Respir. Med. 145 (2018) 145–152, https://doi.org/10.1016/j.rmed.2018.11.004.
[4] X. Zhang, J. Zhang, The human brain in a high altitude natural environment: a review, Front. Hum. Neurosci. 16 (2022) 915995, https://doi.org/10.3389/fnhum.2022.915995.
[5] C. Imray, A. Wright, A. Subudhi, R. Roach, Acute mountain sickness: pathophysiology, prevention, and treatment, Prog. Cardiovasc. Dis. 52 (2010) 467–484, https://doi.org/10.1016/j.pcad.2010.02.003.
[6] F.J. Carod-Artal, High-altitude headache and acute mountain sickness, Neurologia 29 (2014) 533–540, https://doi.org/10.1016/j.nrl.2012.04.015.
[7] E. Pena, S. El Alam, P. Siques, J. Brito, Oxidative stress and diseases associated with high-altitude exposure, Antioxidants 11 (2022) 267, https://doi.org/10.3390/antiox11020267.
[8] N. Xie, F. Fan, S. Jiang, Y. Hou, Y. Zhang, N. Cairang, X. Wang, X. Meng, Rhodiola crenulate alleviates hypobaric hypoxia-induced brain injury via adjusting NF-κB/NLRP3-mediated inflammation, Phytomedicine 103 (2022) 154240, https://doi.org/10.1016/j.phymed.2022.154240.
[9] P. Maiti, S.B. Singh, A.K. Sharma, S. Muthuraju, P.K. Banerjee, G. Ilavazhagan, Hypobaric hypoxia induces oxidative stress in rat brain, Neurochem. Int. 49 (2006) 709–716, https://doi.org/10.1016/j.neuint.2006.06.002.
[10] Q. Shi, J. Fu, D. Ge, Y. He, J. Ran, Z. Liu, J. Wei, T. Diao, Y. Lu, Huperzine A ameliorates cognitive deficits and oxidative stress in the hippocampus of rats exposed to acute hypobaric hypoxia, Neurochem. Res. 37 (2012) 2042–2052, https://doi.org/10.1007/s11064-012-0826-x.
[11] Y. Zhou, X. Huang, T. Zhao, M. Qiao, X. Zhao, M. Zhao, L. Xu, Y. Zhao, L. Wu, K. Wu, R. Chen, M. Fan, L. Zhu, Hypoxia augments LPS-induced inflammation and triggers high altitude cerebral edema in mice, Brain Behav. Immun. 64 (2017) 266–275, https://doi.org/10.1016/j.bbi.2017.04.013.
[12] T.-S. Chang, H.-Y. Ding, S.S.-K. Tai, C.-Y. Wu, Mushroom tyrosinase inhibitory effects of isoflavones isolated from soygerm koji fermented with Aspergillus oryzae BCRC 32288, Food Chem. 105 (2007) 1430–1438, https://doi.org/10.1016/j.foodchem.2007.05.019.
[13] Y.C. Chen, M. Inaba, N. Abe, A. Hirota, Antimutagenic activity of 8-hydroxyisoflavones and 6-hydroxydaidzein from soybean miso, Biosci. Biotechnol. Biochem. 67 (2003) 903–906, https://doi.org/10.1271/bbb.67.903.
[14] R. Tsuchihashi, M. Kodera, S. Sakamoto, Y. Nakajima, T. Yamazaki, Y. Niiho, T. Nohara, J. Kinjo, Microbial transformation and bioactivation of isoflavones from Pueraria flowers by human intestinal bacterial strains, J. Nat. Med. 63 (2009) 254–260, https://doi.org/10.1007/s11418-009-0322-z.
[15] T.S. Chang, Isolation, bioactivity, and production of ortho-hydroxydaidzein and ortho-hydroxygenistein, Int. J. Mol. Sci. 15 (2014) 5699–5716, https://doi.org/10.3390/ijms15045699.
[16] J. Shao, T. Zhao, H.-P. Ma, Z.-P. Jia, L.-L. Jing, Synthesis, characterization, and antiradical activity of 6-hydroxygenistein, Chem. Nat. Compd. 56 (2020) 821–826, https://doi.org/10.1007/s10600-020-03161-5.
[17] A.L. Hopkins, Network pharmacology: the next paradigm in drug discovery, Nat. Chem. Biol. 4 (2008) 682–690, https://doi.org/10.1038/nchembio.118.
[18] L. Zhao, H. Zhang, N. Li, J. Chen, H. Xu, Y. Wang, Q. Liang, Network pharmacology, a promising approach to reveal the pharmacology mechanism of Chinese medicine formula, J. Ethnopharmacol. 309 (2023) 116306, https://doi.org/10.1016/j.jep.2023.116306.
[19] P.C. Fan, H.P. Ma, L.L. Jing, L. Li, Z.P. Jia, The antioxidative effect of a novel free radical scavenger 4'-hydroxyl-2-substituted phenylnitronyl nitroxide in acute high-altitude hypoxia mice, Biol. Pharm. Bull. 36 (2013) 917–924, https://doi.org/10.1248/bpb.b12-00854.
[20] X. Wang, Y. Hou, Q. Li, X. Li, W. Wang, X. Ai, T. Kuang, X. Chen, Y. Zhang, J. Zhang, Y. Hu, X. Meng, Rhodiola crenulata attenuates apoptosis and mitochondrial energy metabolism disorder in rats with hypobaric hypoxia-induced brain injury by regulating the HIF-1α/microRNA 210/ISCU1/2(COX10) signaling pathway, J. Ethnopharmacol. 241 (2019) 111801, https://doi.org/10.1016/j.jep.2019.03.028.
[21] K. Jiang, J. Yang, G. Xue, A. Dai, H. Wu, Fisetin ameliorates the inflammation and oxidative stress in lipopolysaccharide-induced endometritis, J. Inflamm. Res. 14 (2021) 2963–2978, https://doi.org/10.2147/jir.S314130.

[22] D. Li, L. Zhang, X. Huang, L. Liu, Y. He, L. Xu, Y. Zhang, T. Zhao, L. Wu, Y. Zhao, K. Wu, Y. Wu, M. Fan, L. Zhu, WIP1 phosphatase plays a critical neuroprotective role in brain injury induced by high-altitude hypoxic inflammation, Neurosci. Bull. 33 (2017) 292–298, https://doi.org/10.1007/s12264-016-0095-9.
[23] J.V. Lafuente, G. Bermudez, L. Camargo-Arce, S. Bulnes, Blood-brain barrier changes in high altitude, CNS Neurol. Disord.: Drug Targets 15 (2016) 1188–1197, https://doi.org/10.2174/1871527315666160920123911.
[24] S. Jiang, F. Fan, L. Yang, K. Chen, Z. Sun, Y. Zhang, N. Cairang, X. Wang, X. Meng, Salidroside attenuates high altitude hypobaric hypoxia-induced brain injury in mice via inhibiting NF-κB/NLRP3 pathway, Eur. J. Pharmacol. 925 (2022) 175015, https://doi.org/10.1016/j.ejphar.2022.175015.
[25] X. Wang, L. Cui, X. Ji, Cognitive impairment caused by hypoxia: from clinical evidences to molecular mechanisms, Metab. Brain Dis. 37 (2022) 51–66, https://doi.org/10.1007/s11011-021-00796-3.
[26] S. Safe, A. Jayaraman, R.S. Chapkin, M. Howard, K. Mohankumar, R. Shrestha, Flavonoids: structure-function and mechanisms of action and opportunities for drug development, Toxicol. Res. 37 (2021) 147–162, https://doi.org/10.1007/s43188-020-00080-z.
[27] A. Ayala, M.F. Muñoz, S. Argüelles, Lipid peroxidation: production, metabolism, and signaling mechanisms of malondialdehyde and 4-hydroxy-2-nonenal, Oxid. Med. Cell. Longev. 2014 (2014) 360438, https://doi.org/10.1155/2014/360438.
[28] J. Aguilar Diaz De Leon, C.R. Borges, Evaluation of oxidative stress in biological samples using the thiobarbituric acid reactive substances assay, J. Vis. Exp. (2020), https://doi.org/10.3791/61122.
[29] Y. Shen, Z. Shen, P. Li, Z. Chen, B. Wei, D. Liu, X. Si, J. Pan, D. Wu, W. Li, Protective activity of Malus doumeri leaf extract on H(2)O(2)-induced oxidative injury in H9C2 rat cardiomyocytes, Front. Cardiovasc. Med. 9 (2022) 1005306, https://doi.org/10.3389/fcvm.2022.1005306.
[30] J.D. Liu, W.B. Liu, C.Y. Zhang, C.Y. Xu, X.C. Zheng, D.D. Zhang, C. Chi, Dietary glutathione supplementation enhances antioxidant activity and protects against lipopolysaccharide-induced acute hepatopancreatic injury and cell apoptosis in Chinese mitten crab, Eriocheir sinensis, Fish Shellfish Immunol. 97 (2020) 440–454, https://doi.org/10.1016/j.fsi.2019.12.049.
[31] X. Huang, Y. Zhang, B. Qi, K. Sun, N. Liu, B. Tang, S. Fang, L. Zhu, X. Wei, HIF-1α: its notable role in the maintenance of oxygen, bone and iron homeostasis (Review), Int. J. Mol. Med. 50 (2022) 141, https://doi.org/10.3892/ijmm.2022.5197.
[32] S. Movafagh, S. Crook, K. Vo, Regulation of hypoxia-inducible factor-1a by reactive oxygen species: new developments in an old debate, J. Cell. Biochem. 116 (2015) 696–703, https://doi.org/10.1002/jcb.25074.
[33] Z. Zhang, L. Yao, J. Yang, Z. Wang, G. Du, PI3K/Akt and HIF-1 signaling pathway in hypoxia-ischemia (Review), Mol. Med. Rep. 18 (2018) 3547–3554, https://doi.org/10.3892/mmr.2018.9375.
[34] L. Pérez-Gutiérrez, N. Ferrara, Biology and therapeutic targeting of vascular endothelial growth factor A, Nat. Rev. Mol. Cell Biol. 24 (2023) 816–834, https://doi.org/10.1038/s41580-023-00631-w.
[35] X. Yang, Y. Zhang, K. Geng, K. Yang, J. Shao, W. Xia, Sirt3 protects against ischemic stroke injury by regulating HIF-1α/VEGF signaling and blood-brain barrier integrity, Cell. Mol. Neurobiol. 41 (2021) 1203–1215, https://doi.org/10.1007/s10571-020-00889-0.
[36] F. Xu, J.W. Severinghaus, Rat brain VEGF expression in alveolar hypoxia: possible role in high-altitude cerebral edema, J. Appl. Physiol. 85 (1998) 53–57, https://doi.org/10.1152/jappl.1998.85.1.53, 1985.
[37] Y. Zhou, F. Yan, X. Han, X. Huang, X. Cheng, Y. Geng, X. Jiang, Y. Han, M. Zhao, L. Zhu, NB-3 expression in endothelial cells contributes to the maintenance of blood brain barrier integrity in a mouse high-altitude cerebral edema model, Exp. Neurol. 354 (2022) 114116, https://doi.org/10.1016/j.expneurol.2022.114116.
[38] C. Yan, Z. Wang, W. Liu, L. Pu, R. Li, C. Ai, H. Xu, B. Zhang, T. Wang, X. Zhang, Z. Chen, X. Wang, Resveratrol ameliorates high altitude hypoxia-induced osteoporosis by suppressing the ROS/HIF signaling pathway, Molecules 27 (2022) 5538, https://doi.org/10.3390/molecules27175538.
[39] P. Hernansanz-Agustín, J.A. Enríquez, Generation of reactive oxygen species by mitochondria, Antioxidants 10 (2021), https://doi.org/10.3390/antiox10030415.
[40] A.J. Murray, Energy metabolism and the high-altitude environment, Exp. Physiol. 101 (2016) 23–27, https://doi.org/10.1113/ep085317.
[41] J. Li, Y. Qi, H. Liu, Y. Cui, L. Zhang, H. Gong, Y. Li, L. Li, Y. Zhang, Acute high-altitude hypoxic brain injury: identification of ten differential proteins, Neural. Regen. Res. 8 (2013) 2932–2941, https://doi.org/10.3969/j.issn.1673-5374.2013.31.006.
[42] W. Chang, J. Cui, Y. Li, K. Zang, X. Zhang, Z. Zhang, Y. Jiang, Q. Ma, S. Qu, F. Liu, J. Xue, Transcriptomic analysis of the cerebral hippocampal tissue in spontaneously hypertensive rats exposed to acute hypobaric hypoxia: associations with inflammation and energy metabolism, Sci. Rep. 13 (2023) 3681, https://doi.org/10.1038/s41598-023-30682-0.
[43] Y. Hou, F. Fan, N. Xie, Y. Zhang, X. Wang, X. Meng, Rhodiola crenulata alleviates hypobaric hypoxia-induced brain injury by maintaining BBB integrity and balancing energy metabolism dysfunction, Phytomedicine 128 (2024) 155529, https://doi.org/10.1016/j.phymed.2024.155529.
[44] J. Cui, Q. Ma, C. Zhang, Y. Li, J. Liu, K. Xie, E. Luo, M. Zhai, C. Tang, Keratin 18 depletion as a possible mechanism for the induction of apoptosis and ferroptosis in the rat Hippocampus after hypobaric hypoxia, Neuroscience 513 (2023) 64–75, https://doi.org/10.1016/j.neuroscience.2022.11.009.
[45] N. Van Opdenbosch, M. Lamkanfi, Caspases in cell death, inflammation, and disease, Immunity 50 (2019) 1352–1364, https://doi.org/10.1016/j.immuni.2019.05.020.
[46] P.E. Czabotar, G. Lessene, A. Strasser, J.M. Adams, Control of apoptosis by the BCL-2 protein family: implications for physiology and therapy, Nat. Rev. Mol. Cell Biol. 15 (2014) 49–63, https://doi.org/10.1038/nrm3722.
[47] F. He, X. Ru, T. Wen, NRF2, a transcription factor for stress response and beyond, Int. J. Mol. Sci. 21 (2020) 4777, https://doi.org/10.3390/ijms21134777.
[48] P. Shi, Z. Zhan, X. Ye, Y. Lu, K. Song, F. Sheng, H. Shen, P. Yin, The antioxidative effects of empagliflozin on high glucose-induced epithelial-mesenchymal transition in peritoneal mesothelial cells via the Nrf2/HO-1 signaling, Ren, Fail. 44 (2022) 1528–1542, https://doi.org/10.1080/0886022x.2022.2118066.
[49] C. Lisk, J. McCord, S. Bose, T. Sullivan, Z. Loomis, E. Nozik-Grayck, T. Schroeder, K. Hamilton, D.C. Irwin, Nrf2 activation: a potential strategy for the prevention of acute mountain sickness, Free Radic. Biol. Med. 63 (2013) 264–273, https://doi.org/10.1016/j.freeradbiomed.2013.05.024.
[50] G. Gong, L. Yin, L. Yuan, D. Sui, Y. Sun, H. Fu, L. Chen, X. Wang, Ganglioside GM1 protects against high altitude cerebral edema in rats by suppressing the oxidative stress and inflammatory response via the PI3K/AKT-Nrf2 pathway, Mol. Immunol. 95 (2018) 91–98, https://doi.org/10.1016/j.molimm.2018.02.001.
[51] Y. Wang, Z. Shen, C. Pei, S. Zhao, N. Jia, D. Huang, X. Wang, Y. Wu, S. Shi, Y. He, Z. Wang, Eleutheroside B ameliorated high altitude pulmonary edema by attenuating ferroptosis and necroptosis through Nrf2-antioxidant response signaling, Biomed. Pharmacother. 156 (2022) 113982, https://doi.org/10.1016/j.biopha.2022.113982.
[52] S. Aimaier, Y. Tao, F. Lei, Z. Yupeng, S. Wenhui, A. Aikemu, D. Maimaitiyiming, Protective effects of the Terminalia bellirica tannin-induced Nrf2/HO-1 signaling pathway in rats with high-altitude pulmonary hypertension, BMC Compl. Alternative Med. 23 (2023) 150, https://doi.org/10.1186/s12906-023-03981-2.
[53] H. Chen, C. Chen, Y. Qin, L. Wang, J. Zheng, F. Gao, Protective effects of epigallocatechin-3-gallate counteracting the chronic hypobaric hypoxia-induced myocardial injury in plain-grown rats at high altitude, Cell Stress Chaperones (2023), https://doi.org/10.1007/s12192-023-01386-1.
[54] K. Pham, K. Parikh, E.C. Heinrich, Hypoxia and inflammation: insights from high-altitude physiology, Front. Physiol. 12 (2021) 676782, https://doi.org/10.3389/fphys.2021.676782.
[55] S. Malacrida, A. Giannella, G. Ceolotto, C. Reggiani, A. Vezzoli, S. Mrakic-Sposta, S. Moretti, R. Turner, M. Falla, H. Brugger, G. Strapazzon, Transcription factors regulation in human peripheral white blood cells during hypobaric hypoxia exposure: an in-vivo experimental study, Sci. Rep. 9 (2019) 9901, https://doi.org/10.1038/s41598-019-46391-6.
[56] J. Lundeberg, J.R. Feiner, A. Schober, J.W. Sall, H. Eilers, P.E. Bickler, Increased cytokines at high altitude: lack of effect of ibuprofen on acute mountain sickness, physiological variables, or cytokine levels, high, Alt. Med. Biol. 19 (2018) 249–258, https://doi.org/10.1089/ham.2017.0144.
[57] C. Wang, H. Jiang, J. Duan, J. Chen, Q. Wang, X. Liu, C. Wang, Exploration of acute phase proteins and inflammatory cytokines in early stage diagnosis of acute mountain sickness, High Alt. Med. Biol. 19 (2018) 170–177, https://doi.org/10.1089/ham.2017.0126.
[58] P. Liu, L. Pan, L. Cui, T. Li, S. Zhao, Y. Hu, X. Tao, H. Deng, J. Jiang, B. Zhao, Y. Wang, X. Xue, Cordycepin ameliorates acute hypobaric hypoxia induced blood-brain barrier disruption, and cognitive impairment partly by suppressing the TLR4/NF-κB/MMP-9 pathway in the adult rats, Eur. J. Pharmacol. 924 (2022) 174952, https://doi.org/10.1016/j.ejphar.2022.174952.

[59] R. Zelmanovich, K. Pierre, P. Felisma, D. Cole, M. Goldman, B. Lucke-Wold, High altitude cerebral edema: improving treatment options, Biologics (Basel) 2 (2022) 81–91, https://doi.org/10.3390/biologics2010007.
[60] C. Greene, N. Hanley, M. Campbell, Blood-brain barrier associated tight junction disruption is a hallmark feature of major psychiatric disorders, Transl. Psychiatry 10 (2020) 373, https://doi.org/10.1038/s41398-020-01054-3.
[61] Q. Dang, D. Wu, Y. Li, L. Fang, C. Liu, X. Wang, X. Liu, W. Min, Walnut-derived peptides ameliorate d-galactose-induced memory impairments in a mouse model via inhibition of MMP-9-mediated blood-brain barrier disruption, Food Res. Int. 162 (2022) 112029, https://doi.org/10.1016/j.foodres.2022.112029.
[62] T. Lawrence, The nuclear factor NF-kappaB pathway in inflammation, Cold Spring Harbor Perspect. Biol. 1 (2009) a001651, https://doi.org/10.1101/cshperspect.a001651.
[63] M. Karin, M. Delhase, The I kappa B kinase (IKK) and NF-kappa B: key elements of proinflammatory signalling, Semin. Immunol. 12 (2000) 85–98, https://doi.org/10.1006/smim.2000.0210.
[64] Y. He, H. Hara, G. Núñez, Mechanism and regulation of NLRP3 inflammasome activation, Trends Biochem. Sci. 41 (2016) 1012–1021, https://doi.org/10.1016/j.tibs.2016.09.002.
[65] X. Du, N. Amin, L. Xu, B.O.A. Botchway, B. Zhang, M. Fang, Pharmacological intervention of curcumin via the NLRP3 inflammasome in ischemic stroke, Front. Pharmacol. 14 (2023) 1249644, https://doi.org/10.3389/fphar.2023.1249644.